

# THE MIXED PHASE COLLISION ENERGY RANGE FROM THE EXPERIMENTAL DATA\*

MAREK GAZDZICKI

Goethe-University, 60323 Frankfurt am Main, Germany  
and

Institute of Physics, Jan Kochanowski University  
Świętokrzyska 15, 25-406 Kielce, Poland

*(Received October 9, 2014)*

Experimental results on collision energy dependence of relevant hadron production properties are discussed. It is argued that the mixed phase consisting of confined and deconfined matter is created in central Pb+Pb (Au+Au) collisions between  $\approx 8$  and  $\approx 12$  GeV center-of-mass energy of a nucleon–nucleon pair.

DOI:10.5506/APhysPolB.45.2319

PACS numbers: 12.40.–y, 12.40.Ee

## 1. Introduction

The search for the beginning of creation of a deconfined state of strongly interacting matter produced in nucleus–nucleus collisions (the onset of deconfinement) started 20 years ago [1]. A number of signals have been proposed, for review see Ref. [2], and five of them were observed experimentally at low energies of the CERN Super Proton Synchrotron [3, 4]. Today, the relevant data are rich enough to ask the question: at which collision energy does the mixed phase region start and how far does it extend? A semi-quantitative analysis of the results presented here indicates that the mixed phase energy domain in central Pb+Pb (Au+Au) collisions ranges between  $\approx 8$  and  $\approx 12$  GeV center-of-mass energy of as nucleon–nucleon pair.

This paper is based on the talk presented at the 54. Cracow School of Theoretical Physics, “QCD Meets Experiment”.

---

\* Invited talk presented at the LIV Cracow School of Theoretical Physics “QCD Meets Experiment”, Zakopane, Poland, June 12–20, 2014.

## 2. The basic ideas

The search for phase transitions in strongly interacting matter resembles the procedure used to measure the heating curve of water shown in Fig. 1. But instead of measuring the water temperature as a function of heat added, one measures relevant properties of hadrons produced in nucleus–nucleus collisions as a function of collision energy — *the heating curves of strongly interacting matter*.

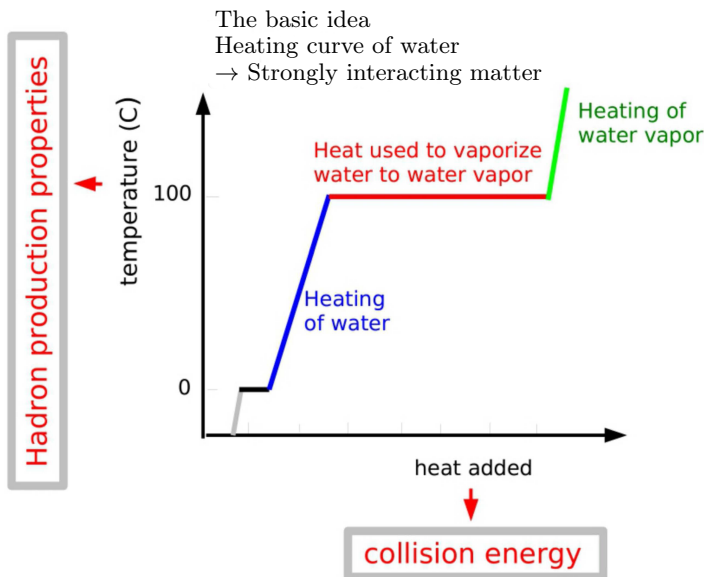


Fig. 1. Analogy between the heating curve of water and heating curves of strongly interacting matter measured via hadron production in heavy ion collisions.

The studies of  $A+A$  collisions are based on the following assumptions:

- System close to equilibrium is created at the early stage of collision.
- Its energy density,  $\varepsilon$ , increases monotonically with increasing collision energy,  $\sqrt{s_{NN}}$ .
- In central Pb+Pb collisions, the system is large enough to model single particle production properties using the grand canonical ensemble.

The experimental procedure to measure *the heating curves of strongly interacting matter* (Fig. 1) makes sense because rich data on nucleus–nucleus collisions are in agreement with models based on the above three assumptions, for review see Ref. [5].

Furthermore one assumes:

- At high enough energy density state of created matter changes (“onset of deconfinement”).
- The change can be modelled by the first order phase transition.

Hence, there are two energies to be measured:

- The beginning of the mixed phase, onset of deconfinement (OD).
- The end of the mixed phase, the softest point (SP).

Thus, by measuring *the heating curves of strongly interacting matter*, one can test assumptions on the existence and nature of phase transitions.

In particular, the Statistical Model of the Early Stage (SMES) [6] of nucleus–nucleus collisions predicts the dependence of the initial matter temperature on collision energy which is qualitatively identical to the corresponding heating curve of water, see Fig. 2.

The example:

SMES  $\cong$   
 Fermi–Landau model  
 + 1<sup>st</sup> order PT  
 M. Gaździcki,  
 M.I. Gorenstein  
 APP B30 (1999) 2705

-----  
 The mixed phase  
 energy range:

$(\sqrt{s_{NN}}$  (OD),  $(\sqrt{s_{NN}}$  (SP))

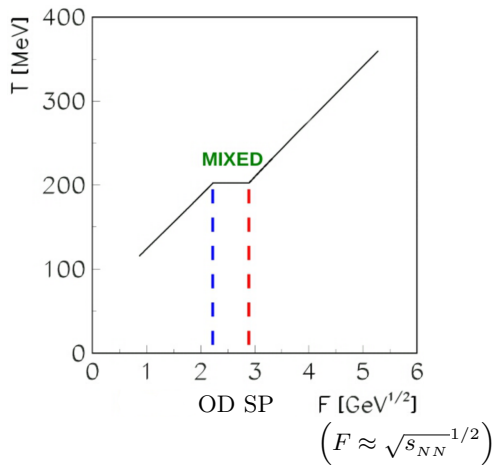


Fig. 2. Schematic heating curve of strongly interacting matter:  $T$  versus collision energy per nucleon pair.

### 3. Onset of deconfinement: experimental evidence

The first two signals of the onset of deconfinement predicted [6] and experimentally observed [3, 4] concern mean multiplicities of pions and kaons. The horn structure (the left plot in Fig. 3) is seen in collision energy dependence of the  $\langle K^+ \rangle / \langle \pi^+ \rangle$  ratio, whereas the kink structure (the right plot in Fig. 3) appears in the energy dependence of  $\langle \pi \rangle / \langle N_W \rangle$  ratio. Here,  $\pi$  stands

for all pions,  $N_W$  for the number of wounded nucleons and  $F$  is the Fermi measure of collision energy [7, 8]. The data on central Pb+Pb and Au+Au collisions are plotted together. The horn structure is visible directly from the data. The kink can be only identified relatively to the model reference — the straight line predicted by the Fermi–Landau model [7, 9].

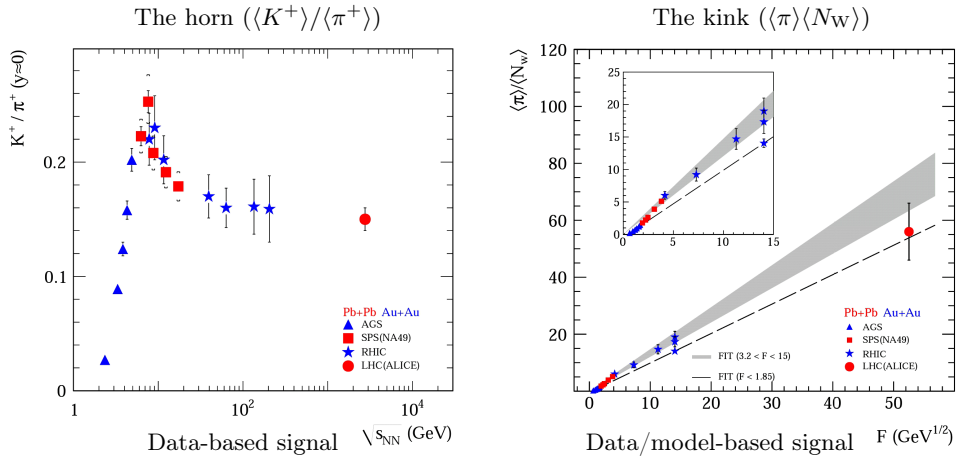


Fig. 3. Experimental evidence for the onset of deconfinement: horn (left) and kink (right) in Pb+Pb and Au+Au collisions.

The next three signals of the onset of deconfinement concern single particle momentum spectra. The step structure [10] (the left plot in Fig. 4) is observed in collision energy dependence of the inverse slope parameter  $T$  of transverse mass spectra. The dale structure [11] (the middle plot in Fig. 4) appears in the energy dependence of the width of rapidity distribution. And the dip structure [12, 13] (the right plot in Fig. 4) refers to the energy dependence of a specific property of azimuthal angle distribution [14]. The data on central Pb+Pb and Au+Au collisions are plotted together. The step and dip structures are visible directly from the data. The dale can be only identified relatively to the model reference — a prediction of the Landau model [9].

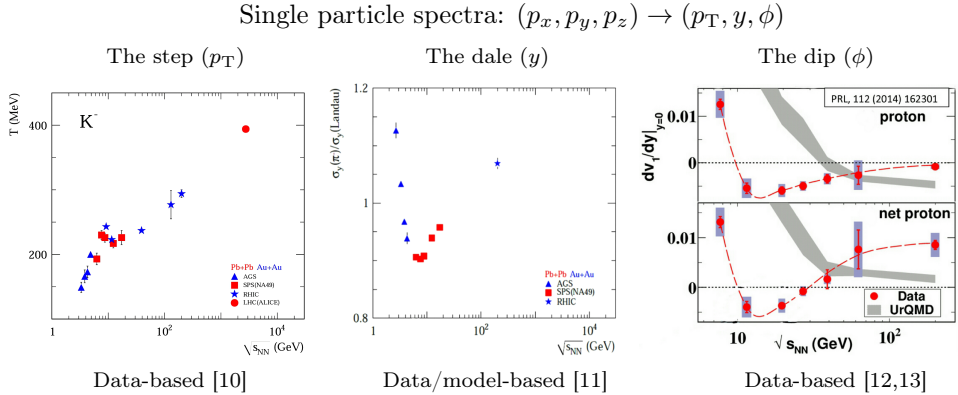


Fig. 4. Experimental evidence for the onset of deconfinement in single particle momentum spectra: inverse slope parameter  $T$  of transverse mass spectra (left), energy dependence of the width of rapidity distribution (middle), specific property of azimuthal angle distribution [14] (right) plotted as functions of collision energy per nucleon pair.

It is easy to understand why the above “2+3” signals of the onset of deconfinement related to single particle properties were proposed and observed:

- |  |              |  |
|--|--------------|--|
| two “material” signals:<br>kink + horn         | $\Leftarrow$ | entropy and strangeness<br>two matter properties<br>sensitive to its state |
| three “motional” signals:<br>step + dale + dip | $\Leftarrow$ | three components of<br>momentum vector                                     |

## 4. The mixed phase region

### 4.1. The mixed phase region: the horn

The energy dependence of the strangeness to entropy ratio (the left plot in Fig. 5) was predicted [6] to have a sharp maximum at the beginning of the mixed phase region, the onset of deconfinement. The ratio is approximately proportional to the  $K^+/\pi^+$  ratio [2]. Thus, the collision energy at which the  $K^+/\pi^+$  ratio has the maximum (the horn, Fig. 5) gives the first estimate of the onset of deconfinement energy. The predicted change at the softest point is less spectacular, and, therefore, a quantitative analysis is needed to estimate the softest point energy.

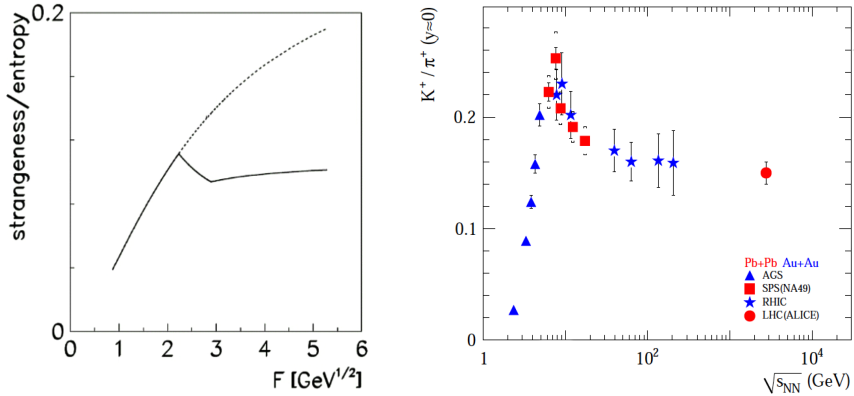


Fig. 5. The energy dependence of the strangeness/entropy and  $K^+/\pi^+$  ratios.

#### 4.2. The mixed phase region: the kink

The energy dependence of the entropy per wounded nucleon (the left plot in Fig. 6) was predicted [6] to increase its slope at the beginning of the mixed phase region. The entropy per wounded nucleon is approximately proportional to the  $\langle \pi \rangle / \langle N_W \rangle$  ratio (see Fig. 3). Thus, the collision energy at which the slope starts to increase (the kink) allows to estimate the energy of the onset of deconfinement [4]. Again, the predicted change at the softest point is less spectacular and, therefore, a quantitative analysis is needed to estimate the softest point energy.

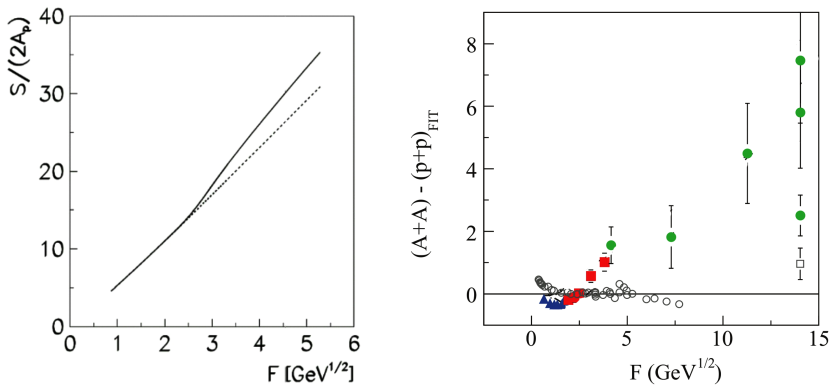


Fig. 6. The energy dependence of the entropy per wounded nucleon and the difference of  $\langle \pi \rangle / \langle N_W \rangle$  ratios measured in Pb+Pb (Au+Au) and  $p+p$  collisions.

4.3. The mixed phase region: the step

The energy dependence of the early stage temperature and the pressure to energy density ratio (the left plots in Fig. 7) was predicted [6] to change significantly twice, at the beginning and at the end of the mixed phase region. The inverse slope parameter of transverse mass spectra of kaons is sensitive to these changes [10]. Thus, the collision energy range at which the  $T$  parameter dependence reveals the changes (the step, right plot in Fig. 7) allows to estimate both the OD and SP energies.

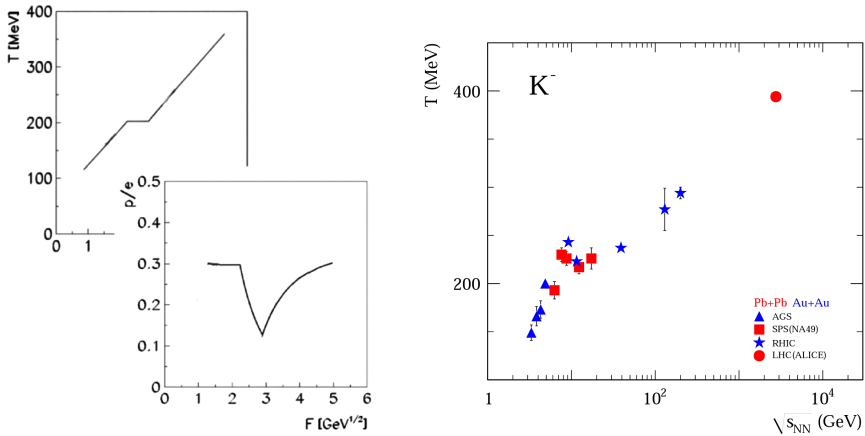


Fig. 7. The energy dependence of the early stage temperature and the pressure to energy density ratio (left) and the inverse slope parameter of  $K^-$  transverse mass spectra in Pb+Pb (Au+Au) collisions.

4.4. The mixed phase region: the dale

The energy dependence of the pressure to energy density ratio (the left plot in Fig. 8) was predicted to change significantly twice, at the beginning and at the end of the mixed phase region. The width of pion rapidity distribution is expected to be sensitive to these changes [11]. Its energy dependence relative to the approximate prediction [15] of the Landau model [9] shows a minimum which can be identified with the softest point. This is shown in the right plot of Fig. 8. The change due to the onset of deconfinement is not observed.

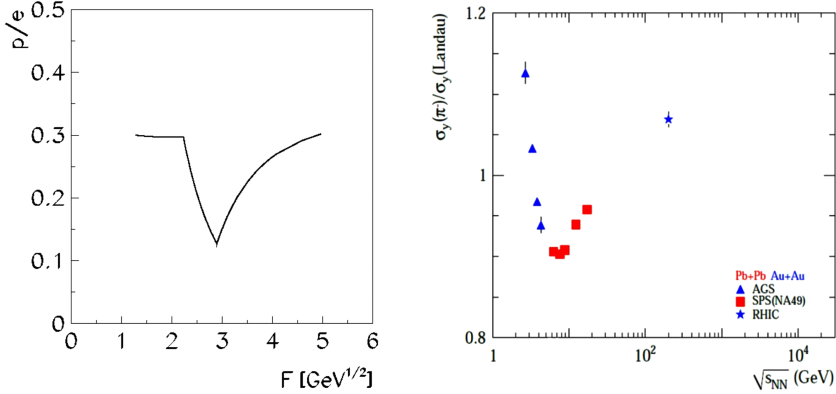


Fig. 8. The energy dependence of the pressure to energy density ratio and ratio of width of pion rapidity distribution to the Landau model prediction.

#### 4.5. The mixed phase region: the dip

The energy dependence of the properties of azimuthal angle distribution (the left plot in Fig 9) was predicted to have a sharp minimum at the end of the mixed phase region [12]. The data show a weak minimum — as shown in the right plot of Fig 9 — which can be identified with the softest point.

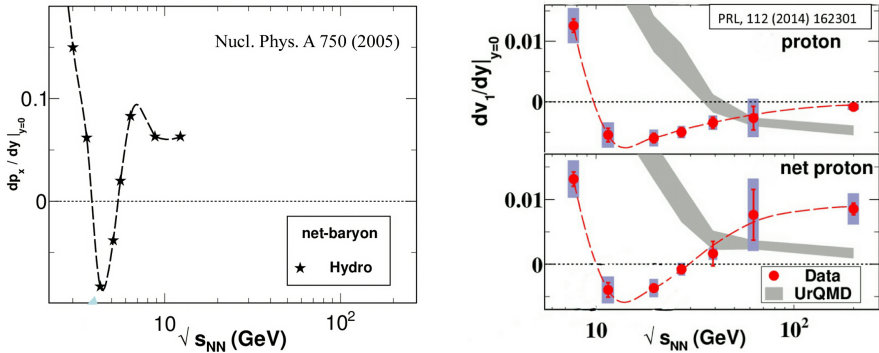


Fig. 9. The energy dependence of a specific property of azimuthal angle distribution model (the left plot) and data (the right plot).

## 5. Summary and conclusions

Estimates of the onset of deconfinement energy and the energy of the softest point extracted from the data discussed in the previous section are summarized in Table I.

TABLE I

The semi-quantitative estimates of the onset of deconfinement and softest point energies in central Pb+Pb (Au+Au) collisions are surprisingly consistent.

Signal	$\sqrt{s_{NN}}$ [GeV]		Comments	
	OD	SP		
Horn	$\approx 8$	—	Data	Mean multiplicities
Kink	$\approx 7$	—	Data/Model	
Step	$\approx 8$	$\approx 12$	Data	Momentum spectra
Dale	—	$\approx 8$	Data/Model	
Dip	—	$\approx 12$	Data	

One can conclude that the onset of deconfinement energy is about 8 GeV and the softest point energy is about 12 GeV as illustrated schematically below. As required by the model used in data analysis, the onset of deconfinement energy is smaller than the softest point one:

$$\sqrt{s_{NN}} \text{ (OD)} \approx 8 \text{ GeV}$$

**MIXED**  $\Updownarrow$  **PHASE**

$$\sqrt{s_{NN}} \text{ (SP)} \approx 12 \text{ GeV}$$

$$(\sqrt{s_{NN}} \text{ (OD)} < \sqrt{s_{NN}} \text{ (SP)} \text{ as it should be)}$$

This work was supported by the National Science Centre of Poland (grant UMO-2012/04/M/ST2/00816) and the German Research Foundation (grant GA 1480/2-2).

## REFERENCES

- [1] M. Gazdzicki, in: Divonne 1994, Hot Hadronic Matter, pp. 215–222; *Z. Phys.* **C66**, 659 (1995).
- [2] M. Gazdzicki, M. Gorenstein, P. Seyboth, *Acta Phys. Pol. B* **42**, 307 (2011) [arXiv:1006.1765 [hep-ph]]; *Int. J. Mod. Phys. E* **23**, 1430008 (2014) [arXiv:1404.3567 [nucl-ex]].
- [3] S.V. Afanasiev *et al.* [NA49 Collaboration], *Phys. Rev.* **C66**, 054902 (2002) [arXiv:nucl-ex/0205002].

- [4] C. Alt *et al.* [NA49 Collaboration], *Phys. Rev.* **C77**, 024903 (2008) [arXiv:0710.0118 [nucl-ex]].
- [5] W. Florkowski, *Phenomenology of Ultra-Relativistic Heavy-Ion Collisions*, Singapore, World Scientific, 2010, p. 416.
- [6] M. Gazdzicki, M.I. Gorenstein, *Acta Phys. Pol. B* **30**, 2705 (1999) [arXiv:hep-ph/9803462].
- [7] E. Fermi, *Prog. Theor. Phys.* **5**, 570 (1950).
- [8] A.I. Golokhvastov, JINR Report E2-89-364 (1989); *Phys. Atom. Nucl.* **64**, 84 (2001) [*Yad. Fiz.* **64**, 88 (2001)].
- [9] L.D. Landau, *Izv. Akad. Nauk Ser. Fiz.* **17**, 51 (1953).
- [10] M.I. Gorenstein, M. Gazdzicki, K.A. Bugaev, *Phys. Lett.* **B567**, 175 (2003) [arXiv:hep-ph/0303041].
- [11] M. Bleicher, arXiv:hep-ph/0509314.
- [12] H. Stoecker, *Nucl. Phys.* **A750**, 121 (2005) [arXiv:nucl-th/0406018].
- [13] L.P. Csernai, D. Rohrich, *Phys. Lett.* **B458**, 454 (1999) [arXiv:nucl-th/9908034].
- [14] L. Adamczyk *et al.* [STAR Collaboration], *Phys. Rev. Lett.* **108**, 202301 (2012) [arXiv:1112.3930 [nucl-ex]].
- [15] E.V. Shuryak, *Yad. Fiz.* **16**, 395 (1972).